Environmental Pollution 269 (2021) 116021

Contents lists available at ScienceDirect

Environmental Pollution

journal homepage: www.elsevier.com/locate/envpol

Structural control of the non-ionic surfactant alcohol ethoxylates (AEOs) on transport in natural soils☆

M. Botella Espeso [a], C. Corada-Fernández [b], M. García-Delgado [b], L. Candela [c], E. González-Mazo [b], P.A. Lara-Martín [b], J. Jiménez-Martínez [a, d, *]

[a] Department of Civil, Environmental and Geomatic Engineering, ETH Zurich, 8093, Zürich, Switzerland
[b] Department of Physical Chemistry, Faculty of Marine and Environmental Sciences, University of Cadiz, Campus of International Excellence of the Sea (CEI•MAR), Río San Pedro, Puerto Real, Cádiz, 11510, Spain
[c] IMDEA Water, Avenida Punto Com 2, Parque Científico Tecnológico Universidad de Alcalá, Alcalá de Henares, 28805, Madrid, Spain
[d] Department of Water Resources and Drinking Water, Eawag, 8600, Dübendorf, Switzerland

ARTICLE INFO

Article history:
Received 31 May 2020
Received in revised form
13 September 2020
Accepted 5 November 2020
Available online 9 November 2020

ABSTRACT

Surfactants, after use, enter the environment through diffuse and point sources such as irrigation with treated and non-treated waste water and urban and industrial wastewater discharges. For the group of non-ionic synthetic surfactant alcohol ethoxylates (AEOs), most of the available information is restricted to the levels and fate in aquatic systems, whereas current knowledge of their behavior in soils is very limited. Here we characterize the behavior of different homologs (C12–C18) and ethoxymers (EO3, EO6, and EO8) of the AEOs through batch experiments and under unsaturated flow conditions during infiltration experiments. Experiments used two different agricultural soils from a region irrigated with reclaimed water (Guadalete River basin, SW Spain). In parallel, water flow and chemical transport were modelled using the HYDRUS-1D software package, calibrated using the infiltration experimental data. Estimates of water flow and reactive transport of all surfactants were in good agreement between infiltration experiments and simulations. The sorption process followed a Freundlich isotherm for most of the target compounds. A systematic comparison between sorption data obtained from batch and infiltration experiments revealed that the sorption coefficient (K_d) was generally lower in infiltration experiments, performed under environmental flow conditions, than in batch experiments in the absence of flow, whereas the exponent (β) did not show significant differences. For the low clay and organic carbon content of the soils used, no clear dependence of K_d on them was observed. Our work thus highlights the need to use reactive transport parameterization inferred under realistic conditions to assess the risk associated with alcohol ethoxylates in subsurface environments.

EscuLeer fonétic.

Main findings

AEOs sorption coefficients were lower and with less variability in infiltration than batch experiments. Similar behavior in natural systems between homologs and between ethoxymers. No dependence of sorption coefficient on low clay and organic carbon content.

Diccionario - Ver diccionario detallado.

1. Introduction

Surfactants are among the most widely used synthetic chemicals globally, with applications in the formulation of pesticides, paints, pharmaceuticals, wetting agents, pulp and paper industries, and personal care products, among many others, but their main use is in the formulation of domestic and industrial detergents. After use, surfactants enter the environment through diffuse, *e.g.*, runoff, and point sources, mainly from urban and industrial wastewater discharges. Although the removal rate of most these compounds during wastewater treatment is often very high (95–99%; Matthijs

☆ This paper has been recommended for acceptance by Dr. Yong Sik Ok.

* Corresponding author. Department of Water Resources and Drinking Water, Eawag, 8600, Dübendorf, Switzerland.
E-mail addresses: joaquin.jimenez@eawag.ch, jjimenez@ethz.ch (J. Jiménez-Martínez).

https://doi.org/10.1016/j.envpol.2020.116021

et al., 1999; McAvoy et al., 1998), they can reach terrestrial environments through irrigation using reclaimed water or application of sludge as fertilizer in agriculture (Topp et al., 2012). As a result of their widespread and high volume of use, surfactants have been detected in a variety of continental and marine aquatic systems (González-Mazo et al., 1998, 2002; León et al., 2001). Most of the studies focused on the anionic linear alkylbenzene sulfonates (LAS) (Eichnorn et al., 2002; Carlsen et al., 2002; Ding et al., 1999) and the non-ionic alkylphenol ethoxylates (APEOs) (Jonkers et al., 2003; Ferguson et al., 2001). Their presence and fate in subsurface environments have received been widely studied. In aquifers, the degradation of alkylphenol ethoxylates has been detected, producing ethoxycarboxylated alkylphenols and alkylphenols (Ahel et al., 1996; Montgomery-Brown et al., 2003; Guang-Guo, 2006; Tubau et al., 2010), which are estrogenic. The presence of sulfophenyl carbolic acids derived from linear alkylbenzene sulfonate degradation has also been detected in groundwater (Krueger et al., 1998; Tubau et al., 2010). However, the characterization of their percolation has received less attention. Percolation experiments performed for LAS shown that their retention was favored by higher clay and organic matter contents (McAvoy et al., 1994; Küchler and Schnaak, 1997; Boluda et al., 2010). In the case of biodegradation within the soil column, > 25% of LAS was removed, reducing percolation to deeper layers.

Here we focus on alcohol ethoxylates (AEOs), which are another important group of non-ionic surfactants that are commonly used in domestic and commercial detergents, household cleaners and personal care products (Droge and Hermens, 2007; Hermens and Droge, 2009). AEOs are efficiently removed (up to 99%) in wastewater treatment plants by a combination of sorption onto sludge and aerobic degradation (Szymanski et al., 2003; Wind et al., 2006), with total AEO concentrations in the effluents ranging from 0.92 to 22.7 μg/L in Europe and North America (Eadsforth et al., 2006; Morrall et al., 2006). Once in the environment, their behavior is controlled by further sorption and degradation processes. AEOs are found dissolved and associated with particulate material, with previous field measures suggesting that up to 86% of the total measured concentration is found sorbed on suspended solids (Lara-Martín et al., 2008). Partition coefficients have been measured ranging from 40 to 7000 L/kg (Cano and Dorn, 1996; Kiewiet et al., 1996; Van Compernolle et al., 2006; Droge et al., 2009), depending on the polarity and sorption capacity of the different AEO homologs and ethoxymers. Most of these studies characterized the sorption of these surfactants using very high concentrations, of several ppm (up to 2000 ppm) (Podoll et al., 1987). However, in the environment, these chemicals are found at much lower concentrations, *e.g.*, in the water column they are usually in the low ppb range (Lara-Martín et al., 2011). Furthermore, most of the available information is restricted to the levels and fate of AEOs in aquatic systems (Petrovic et al., 2002; Lara-Martín et al., 2005, 2008, 2014; Corada-Fernández et al., 2011, 2013). Natural abatement of AEOs occur in terrestrial environments due to a combination of biodegradation and sorption, delaying the arrival of these contaminants in aquifers and minimizing, but not eliminating (García et al., 2019), the risk of groundwater pollution (Durán-Álvarez et al., 2014; Corada-Fernández et al., 2017). However, current knowledge of their behavior in soils is limited. Some of the works carried out in soils have been mainly focus on the ability of non-ionic surfactants to solubilize relatively insoluble contaminants such as hydrocarbons (*e.g.*, Lee et al., 2000; Haigh, 1996). The sorption of non-ionic surfactants in soils have been characterized for following a Langmuir isotherm (Lee et al., 2005) and two-sorption regimes (Adeel and Luthy, 1995). A competition between AEOs homologs for adsorption sites has also been described (Droge and Hermens, 2010). A high correlation with soil mineral properties has been observed (Lee et al., 2005), as well as a much greater role of the chain length of AEOs in the interaction (association) with humic substances as compared to the ethoxylate group member (McAvoy and Kerr, 2001).

Understanding the coupling of natural abatement and transport of AEOs in soils is determinant for predicting their mobility and leaching to groundwater. We here describe laboratory experiments to quantify the fate and transport of AEOs in two natural soils, using a variety of AEOs to represent the wide structural diversity of commercial products, which include compounds with different numbers of carbon atoms in their hydrophobic alkyl chain bonded to a hydrophilic chain with a varying number of ethoxylate units. By combining batch and infiltration experiments, we are able to compare parameters estimated in the absence of flow in batch experiments, with those obtained under realistic environmental flow conditions in infiltration experiments. The use of a numerical solver to simulate the non-equilibrium chemical transport of the targeted compounds allowed us to parameterize the sorption of AEOs under real environmental conditions.

2. Materials and methods

2.1. Characterization of soil samples

Soil samples were taken from two locations, locally known as Rio Viejo (soil core 1) and Guadalcacín (soil core 2), in a region where agricultural soils are irrigated with reclaimed water and amended using sludge, after being composted (Guadalete River basin, SW Spain) (Biel-Maeso et al., 2017). Soil physical properties were determined with respect to depth using a series of techniques and standards (Table 1). The grain size distribution was determined according to ASTM D 422-63 and Gee and Or (2002). Soil textural class was defined according to the USDA system. Bulk density was determined following Grossman and Reinsch (2002). Saturated hydraulic conductivity, which can be highly affected by the concentration of surfactants in the solution, was empirically determined in the laboratory (Reynolds and Elrick, 2002). Organic carbon (OC) content was determined by dichromate oxidation, following Gaudette et al. (1974) and the modification proposed by El Rayis (1985).

2.2. Infiltration experiments

Infiltration experiments were performed in *quasi* two-dimensional flow cells (495 mm × 587 mm × 10 mm, see Fig. 1). One flow cell was filled for each soil sample, maintaining the natural order and thickness of their horizons and the original bulk density (Table 1). The base of each flow cell was filled with silica sand (Ottawa sand) to ensure drainage. Infiltration experiments lasted 192 h for soil core 1, and 69 h for soil core 2, and were conducted at constant temperature (20 °C). An AEO solution consisting of a mixture of homologs (C12, C14, C16, and C18) and their corresponding ethoxymers (3, 6 and 8 EO ethoxylated groups) (Sigma-Aldrich) at 100 ng/cm^3 (100 ppb) was injected for the duration of the experiments at a constant flow rate (0.083 and 0.43 cm^3/h for soil 1 and 2, respectively) using a peristaltic pump and an evenly drip irrigation system. The goal is to characterize the general behavior of AEOs and the control of their structural diversity under different environmental conditions, including flow conditions and soil types, rather than a systematic comparison between soil types. The applied concentration of AEOs mimics previously recorded environmental conditions. The applied solution contained the same concentration of cations (SAR = 5.31) as the original interstitial water of the soil, with pH [8–8.3], electrical

Table 1
Physico-chemical and hydraulic properties of soil cores 1 and 2. OC is the soil organic carbon content; ρ_b is the bulk density; θ_r, and θ_s are the residual and saturated water content, respectively; α is the inverse of the air entry value; n is the pore size distribution index; K_s is the saturated hydraulic conductivity; and λ is the dispersivity of solute in each soil horizon.

Horizon	Depth	Texture [%]			OC [%]	ρ_b	Soil type	θ_r	θ_s	α	n	K_s	λ
	[cm]	Sand	Silt	Clay		[g/cm^3]		[cm^3/cm^3]	[cm^3/cm^3]	[1/cm^1]	[-]	[cm/h]	[cm]
1A	0–19	41.71	54.68	3.61	1.1	1.3349	Silty loam	0.0343	0.3638	0.0091	1.5477	2.67	0.6
1B	19–30.5	84.42	14.58	1	0.3	1.5154	Loamy sand	0.0392	0.3739	0.0436	2.1783	8.97	1.87
1C	30.5–47.1	100	0	0	0	1.9438	Sand	0.049	0.2663	0.0295	4.036	26.23	1.3
2A	0–14	64.36	33.29	2.35	1.2	1.6499	Sandy loam	0.0277	0.3639	0.0507	1.3946	1.50	2.37
2B	14–18.5	46.4	51.88	1.72	0.6	1.6868	Silt loam	0.0252	0.427	0.0319	1.3423	0.95	3.04
2C	18.5–29.5	41.17	54.77	4.06	0.6	1.7095	Silt loam	0.0277	0.3557	0.0245	1.3515	0.66	3.04
2D	29.5–46.5	100	0	0	0	2.0098	Sand	0.0492	0.2563	0.0288	4.1103	23.62	1.3

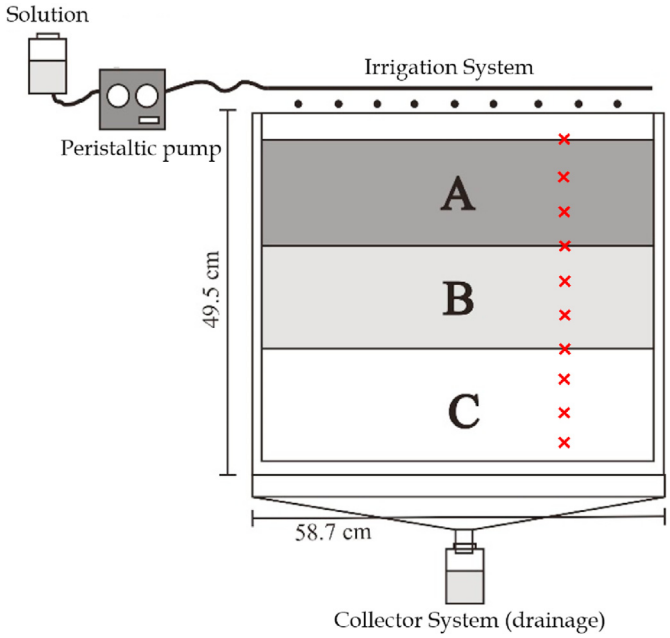

Fig. 1. Schematic of the flow cell for the infiltration experiments. A drip irrigation system provided a solution containing a mixture of AEOs at a constant flow rate throughout the experiments. The collector system provided drainage. Soil horizons (shading) and sample points (red crosses) are shown for soil core 1.

conductivity [500–800] μS/cm, and cation-exchange capacity [32–35] mmol/kg (Corada-Fernandez et al., 2015). Soil and water samples were collected at the same depths throughout the profile of the flow cell before and after the experiments in order to characterize the mobility of the targeted compounds. The concentration of AEOs in both phases was analyzed following Lara-Martín et al. (2006, 2012), providing measures of water content and total concentrations (sorbed + dissolved) of the contaminants at each selected depth.

2.3. Batch experiments

Sorption isotherms were determined using conventional batch experiments following the OECD 106 guidelines, as previously reported for characterizations of the sorption of AEOs onto marine sediments (Traverso-Soto et al., 2014). Briefly, for each soil horizon, 0.5 g of freeze-dried soil were placed in 80 mL polypropylene tubes and stirred together with 50 mL of sterilized water containing different concentrations of AEO homologs (C12, C14, C16, and C18) and their corresponding ethoxymers (3, 6 and 8 EO ethoxylated groups) (5, 10, 25, 50, 100, and 200 ng/cm^3) for 24 h. The aqueous phase was separated from the soil by centrifugation (30 min at 20,000 *g*) and analyzed following Lara-Martín et al. (2006, 2012). Sorption of AEOs by the particulate phase was quantified as the difference between the initial concentration in solution and that measured at the end of the experiment. Control experiments were also performed to check for the biodegradation of AEO homologs, the sorption to the walls of the containers used, and the possible contribution of soils to the mass of AEO added, resulting all of them being negligible (< 1%).

2.4. Modelling reactive transport

To simulate the water flow and reactive transport of the AEO homologs and ethoxymers during the infiltration experiments, the HYDRUS-1D code was used (Šimůnek et al., 2015). Flow and transport equations described below are solved by the software numerically using standard Galerkin-type linear finite element schemes subjected to appropriate initial and boundary conditions (Šimůnek et al., 2015).

2.4.1. Variably saturated flow

For uniform one-dimensional flow in a partially saturated porous medium, and assuming that the gas phase does not play a significant role in the flow of the liquid phase, the equation governing the flow is given by the following modified Richards expression:

$$\frac{\partial\theta}{\partial t}=\frac{\partial}{\partial x}\left[K\left(\frac{\partial h}{\partial x}+1\right)\right]-S \quad (1)$$

where θ is the volumetric water content [L^3 L^{-3}], h the soil pressure head [L], S the sink term [T^{-1}], x the spatial coordinate in the vertical direction [L], and t the time [T]. K is the unsaturated hydraulic conductivity [L T^{-1}], and is as follows:

$$K(h,z)=K_s(x)K_r(h,x) \quad (2)$$

where K_r is the relative hydraulic conductivity and K_s the saturated hydraulic conductivity [L T^{-1}].

Water retention and unsaturated hydraulic conductivity functions of each soil layer were obtained from the constitutive equation of van Genuchten–Mualem (Mualem, 1976; Van Genuchten, 1980)

$$\theta(h)=\begin{cases}\theta_r+\dfrac{\theta_s-\theta_r}{\left[1+|\alpha h|^n\right]^{1-1/n}} & h<0\\ \theta_s & h\geq 0\end{cases} \quad (3)$$

$$K(h) = K_s S_e^l \left\{ 1 - \left[1 - S_e^{n/(n-1)} \right]^{1-1/n} \right\}^2 \quad (4)$$

where S_e is the effective saturation

$$S_e = \frac{\theta(h) - \theta_r}{\theta_s - \theta_r} \quad (5)$$

and $\theta(h)$ the volumetric water content at pressure head h, *i.e.*, water retention function. The parameters θ_r and θ_s are the residual and saturated water content, respectively, α is the inverse of the air entry value, n is the pore size distribution index, and l is a pore-connectivity parameter. In order to reduce the number of parameters, l is commonly assumed to be 0.5, *e.g.*, Mualem (1976). Initial values of these parameters were estimated using ROSETTA (Schaap et al., 2001), a pedotransfer function model that predicts hydraulic parameters from soil texture (% of sand, silt, and clay) and related data. In this case, we also consider the soil bulk density, ρ_b (Table 1).

2.4.2. Reactive transport

The transport equation, including the advection-dispersion processes, and degradation and sorption as reactive processes:

$$\frac{\partial \theta C_w}{\partial t} + \frac{\partial \rho_b C_s}{\partial t} = \frac{\partial}{\partial x}\left(\theta D \frac{C_w}{\partial x} \right) - \frac{\partial q C_w}{\partial x} - \mu \theta C_w \quad (6)$$

where C is the chemical concentration [M L^{-3}], with subscripts w and s for the concentration in the interstitial water and sorbed in the solids, respectively; q is the water flux [LT^{-1}]; μ is the degradation constant for the chemical in liquid phase [T^{-1}]; and ρ_b is the bulk density of the soil [M L^{-3}]. D is the dispersion coefficient [L^2 T^{-1}] following Bear (1972):

$$\theta D = \lambda |q| + \theta D_m \tau_w \quad (7)$$

where D_m is the molecular diffusion coefficient [L^2 T^{-1}]; τ_w is the tortuosity, computed as $\tau_w = \theta^{7/3}/\theta_s^2$ following Millington and Quirk (1961); $|q|$ is the absolute value of flux [L T^{-1}]; and λ the longitudinal dispersivity [L].

The isotherm of sorption that relates C_s and C_w is defined as

$$C_s = \frac{K_d C_w^\beta}{1 + \eta C_w^\beta} \quad (8)$$

where K_d [L^3M^{-1}], β [-] and η [L^3M^{-1}] are the coefficients of the isotherm. The isotherms of Freundlich, Langmuir and the linear isotherm are specific cases: with $\beta = 1$ the isotherm is that of Langmuir, with $\eta = 0$ the isotherm is that of Freundlich, while with both $\beta = 1$ and $\eta = 0$ the isotherm is linear.

2.4.3. Scaling of the hydraulic properties

The effect of changes in concentration on surface tension and viscosity, and consequently on water retention (pressure–water saturation) and hydraulic conductivity functions, were considered using Smith and Gillham's (1994, 1999) scale relationships. From the capillary pressure–surface tension ratio, the effect of a solution on the pressure–saturation ratio can be predicted from the relationship between the surface tension of pore water as a function of concentration (σ) and the surface tension for pure water (σ_o)

$$h(\theta, C_w) = \frac{\sigma}{\sigma_o} h(\theta, C_{wo}) \quad (9)$$

where $h(\theta,C_{wo})$ is the pressure for a water content and a reference concentration C_{wo} (C_{wo} is 0 for pure water), and $\mathbf{h}(\theta,C_w)$ is the soil pressure head scaled to the same water content and concentration.

The hydraulic conductivity as a function of concentration $\mathbf{K}(\theta,C_w)$ is computed from the relation between viscosity of the solution and pure water as

$$K(\theta, C_w) = \frac{v}{v_o} K(\theta, C_{wo}) \quad (10)$$

where $\mathbf{K}(\theta,C_w)$ is the concentration-dependent unsaturated hydraulic conductivity obtained from the hydraulic conductivity for pure water at the same water content $K(\theta,C_{wo})$ and according to the relative viscosity v/v_o, v is the viscosity of pore water as a function of concentration and v_o is the viscosity for pure water.

2.4.4. Modelling setup: initial and boundary conditions

The flow cells used for infiltration experiments were discretized with 90 equidistant nodes separated by 0.5 cm. Three and four different layers were considered for soil core 1 and 2, respectively, while the mass balance was defined for the whole system. Each soil horizon was assigned an initial water content and concentration of the homologs (C12, C14, C16, and C18) and their corresponding ethoxymers (3, 6 and 8 EO ethoxylated groups). We assumed no hysteresis in the water retention functions. As boundary conditions for the water flow, constant flow at the surface (q = 0.083 mL/min and q = 0.43 mL/min for soil core 1 and 2, respectively) and free drainage at the bottom were imposed. No evaporation was considered at the upper limit. For transport, variable concentration and free drainage were assumed at the upper and lower limit, respectively. A direct simulation was performed to solve unsaturated flow in both infiltration experiments. The inverse method was applied to parameterize the reactive transport processes, in particular the sorption process (K_d, β and η, Eq. (8)), and compare the values obtained under actual infiltration conditions with those inferred from batch experiments.

The parameterization of the reactive transport of the AEOs was completed with the dispersivity (λ) for each soil horizon, which was obtained from the literature for the same texture and scale, *i.e.*, soil horizon thickness (Table 1) (Vanderborght and Vereecken, 2007). The same molecular diffusion coefficient $D_m = 1.008 \times 10^{-2}$ cm^2/h (Song et al., 2006) was used for all contaminants, and a degradation constant μ (1/h) for each of them (Hermens and Droge, 2009) (Table 2). The μ values used were slightly higher (*i.e.*, shorter half-life) than the ones provided for similar compounds (*e.g.*, linear alcohol ethoxylates) in a large variety of soils (Knaebel et al., 1990; Federle et al., 1997), although within the same order of magnitude. Note that for the numerical simulations μ includes natural decay and biodegradation. The first order sorption rate coefficient (k) for

Table 2
Degradation constant μ of the alcohol ethoxylates used in the experiments (from Hermens and Droge, 2009).

Hydrocarbon chain	EO group	μ
		[1/h]
C12	EO3	0.1733
	EO6	0.0866
	EO8	0.0578
C14	EO3	0.1733
	EO6	0.0866
	EO8	0.0866
C16	EO3	0.1733
	EO6	0.0866
	EO8	0.0866
C18	EO3	0.0866
	EO6	0.1733
	EO8	0.1733

one site or two sites non-equilibrium sorption, *i.e.*, the mass transfer coefficient for solute exchange between mobile and immobile liquid regions, was estimated as having an average value of $k = 6.5$ 1/h, with a small variability between surfactants; therefore, the same value was used for all of them.

The transport regime was characterized by two dimensionless numbers, the Péclet number and the Damköhler number. The Péclet number (Pe) represents the relative importance of advective (τ_a) and diffusive (τ_d) effects during transport. Here, we compute it as $Pe = \tau_d/\tau_a = (u/D_m)\Delta x$ (El-Kadi and Ge, 1993), where u is the mean water velocity ($u = q/\theta$), and Δx the spatial discretization (0.5 cm in this case). The relative importance of transport to chemical reactions is measured by the Damköhler number (Da), representing the ratio of advection (τ_a) to reaction (τ_r) timescales, $Da = \tau_a/\tau_r$. The reaction timescale is defined by the kinetics of sorption (k) in well-mixed conditions $\tau_r = 1/(C_{wo}k)$ (Connors 1990). Chemical reactions can thus be classified as mixing-driven (or mixing-limited), when the reaction is fast compared to advection ($Da \gg 1$), or kinetics-driven ($Da \ll 1$).

3. Results

3.1. Model calibration: flow and reactive transport

Simulations using HYDRUS-1D with the ROSETTA initial hydraulic parameter estimates yielded water content profiles for both soil cores in the infiltration experiments that were in good agreement with the experimental data (Fig. 2). Transitions between soil horizons are clearly identified with abrupt changes in water content. The use of parameter optimization routines of HYDRUS-1D to calibrate the soil hydraulic parameters did not improve the goodness-of-fit of the direct simulations. The influence of surfactant structures on the equilibrium surface properties, and sorption behaviors at the air–water interface have been investigated systematically (Kanokkarn et al., 2017). At very low concentrations, AEOs are maintained almost at the same surface tension equilibrium level as pure water. For the surfactant concentration used in these experiments, the impact on surface tension is negligible. Consequently, no changes in the hydraulic properties by the presence of surfactants were considered.

The set of hydraulic parameters was subsequently used to parametrize, using optimization routines of HYDRUS-1D, the isotherm of sorption (Eq. (8)) for each surfactant in each soil horizon. The average Pe and Da were both less than 1, so that an equilibrium or quasi-equilibrium model was assumed, *i.e.*, the sorption process was considered to be a fast-reversible reaction. The reactive transport of the twelve targeted AEOs in each flow cell was simulated to characterize their sorption under realistic conditions. Fig. 3 shows a final total concentration ($C_s + C_w$) profile for C14AEO8 as an example. Profiles for the other compounds are shown in Figure S1 and S2, Supplementary Material.

Overall, there was good agreement between the measured concentrations at the different depths in the infiltration experiments and the HYDRUS-1D predictions at the same depths (Table 3). The use of the coefficient of determination (R^2) was discarded because it is insensitive to additive and proportional differences between the model simulations and observations, *i.e.*, large values of R^2 can be obtained even when the model-simulated vales differs considerably in magnitude and variability from the observed ones. Instead, a dimensionless measure, the coefficient of efficiency (E), also called Nash-Sutcliffe model efficiency coefficient (Nash and Sutcliffe, 1970), can provide a relative assessment of the model performance. The root mean square error (*RMSE*) was systematically greater than the mean absolute error (*MAE*), indicating the presence of outlier values. As a consequence, we employ a modified coefficient of efficiency (E'), in which the errors and differences (between measured and simulated) are given their appropriate weighting, rather than being inflated by their squared values (Legates and McCabe, 1999; Ritter and Muñoz-Carpena, 2013). The criteria is as follow: $E' = 1$ when the model fits the data perfectly; $E' = 0$ when the model provides predicted values that are as accurate as using the mean of the observations; and $E' <$

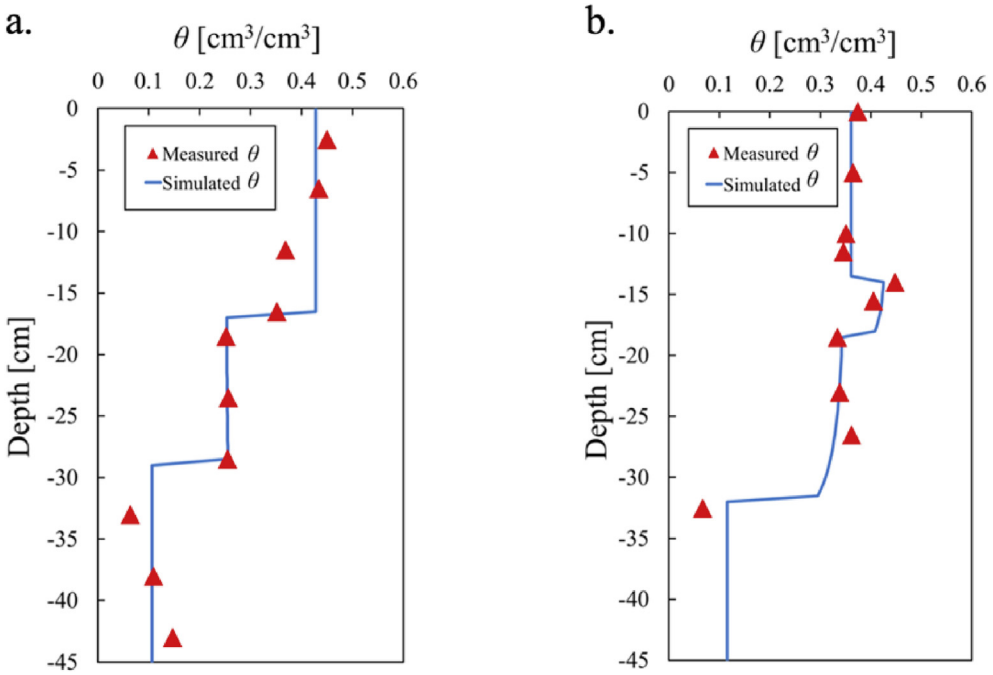

Fig. 2. Soil water content θ [cm^3/cm^3] with depth measured in the infiltration experiments (triangles) and simulated using HYDRUS-1D with the ROSETTA hydraulic parameter estimates (solid line). Values are shown for soil core 1 (a) and soil core 2 (b), 192 and 69 h, respectively, after the start of the experiments.

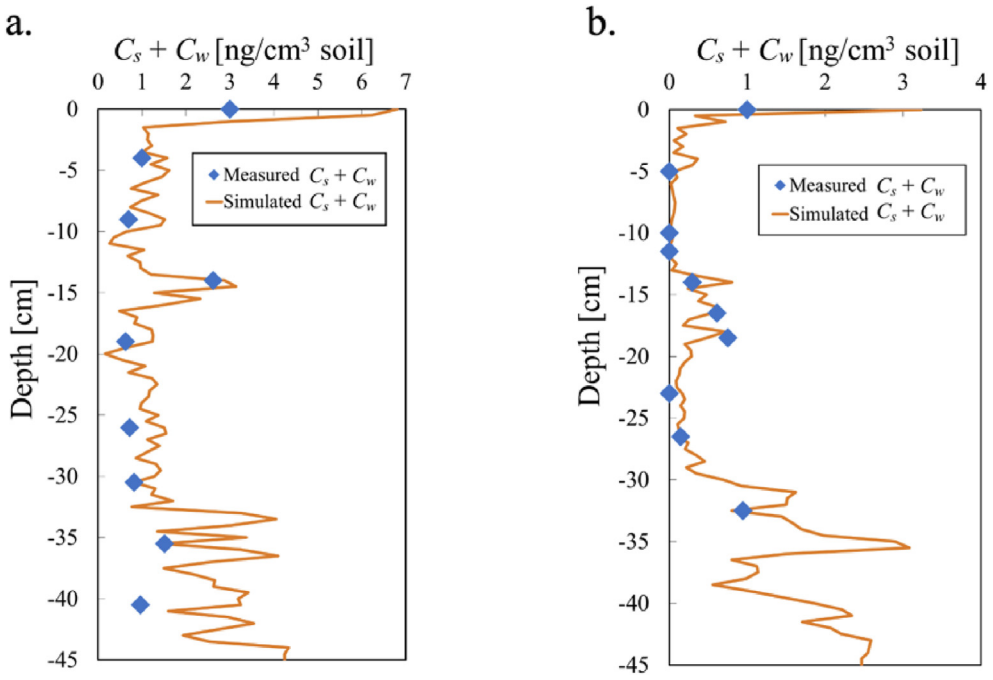

Fig. 3. Total concentration ($C_s + C_w$) [ng/cm^3 of soil] of C14AEO8 measured at different depths in the infiltration experiments (rhomboids) and simulated using HYDRUS-1D (solid line). Values are shown for soil core 1 (a) and soil core 2 (b), 192 and 69 h, respectively, after the start of the experiments.

0 when the model predictions are worse than using the mean of the observations. Values of *E'* for our model indicated a very good fit for soil water content predictions, and an acceptable fit for the total concentration ($C_s + C_w$) predictions for each compound, with some close to 0 and a few lower than 0 (Table 3).

3.2. Sorption isotherms: measured vs. simulated

In both batch experiments and numerical simulations, the Freundlich isotherm was the best reproducing the sorption process of the AEOs, in agreement with previous studies (Brownawell et al., 1997; John et al., 2009). Values of K_d, describing the coefficient of the sorption isotherm, for C12, C14 and C18 from batch experiments ranged from 1.62×10^{-7} to 1.96×10^{-5} cm^3/ng, while values for C16 ranged from 8.51×10^{-7} to 3.8×10^{-6} cm^3/ng (Fig. 4a). In contrast, K_d values obtained from simulations had a narrower range, with values between 3.72×10^{-8} and 4×10^{-7} cm^3/ng. When considered as a function of the number of ethoxylated groups, for batch experiments, EO3 shows a narrower range than EO6 and EO8, between 7.47×10^{-7} and 5.89×10^{-6} cm^3/ng, but, as for carbon chain length, the simulated K_d value was very similar for all of them (Fig. 4b). In general, simulated K_d values were between 1 and 2 orders of magnitude smaller than those measured in batch experiments.

Values of β obtained from batch experiments as a function of the length of the carbon chain range from 0.6 to 2, while those from the simulations range from 0.6 to 0.95 (Fig. 4c). Overall, similar β values were obtained from batch experiments and simulation of the infiltration experiments, although there were deviations from the line 1:1, most noticeable for values for ethoxymers with 3 EO groups (Fig. 4d) derived from batch experiments.

3.3. Dependence of K_d on clay and organic carbon

A dependence of sorption on the soil clay and organic carbon content has been reported in previous works (Shen, 2000; Traverso-Soto et al., 2014), with the following relationships: (*i*) sorption increases with the number of ethoxylated groups as clay content increases, and (*ii*) sorption increases with the carbon chain length as organic carbon content increases. In our batch experiments, in contrast, there was an almost stable K_d value of around 4×10^{-6} cm^3/ng for clay content > 1%, regardless of the number of ethoxylated groups (Fig. 5a). Similarly, K_d values reached an asymptote of 3.16×10^{-6} cm^3/ng for organic carbon content > 0.3%, regardless of the carbon chain length (Fig. 5b). An almost constant value of K_d as function of clay and organic carbon content, although of lower magnitude, was observed for the simulated values ($K_d \sim 1 \times 10^{-7}$ cm^3/ng).

4. Discussion

The direct flow model, *i.e.*, using hydraulic parameters estimated from ROSETTA, captured well the hydrodynamics in both infiltration experiments. A calibration by inverse method of the hydraulic parameters (using the available water content measurements) did not improve the fit. This, along with the plausibility of the model parameters, indicated the appropriateness of the flow parameterization (Fig. 2). To assess the appropriateness of the adopted transport-related parameters, a sensitivity analysis for the dispersivity values taken from the literature (Vanderborght and Vereecken, 2007) demonstrated the low impact on the conservative and reactive transport results. Note that the ranges of dispersivity values used were smaller than one order of magnitude due to the thickness of the soil horizons and the numerical spatial discretization adopted.

HYDRUS-1D (Šimůnek et al., 2015) has been extensively used to solve sorption and the coupled transport in pore domains with different advective velocities, providing accurate simulations when compare with a number of numerical models (Vanderborght et al., 2005). The reactive transport model was based on the flow and conservative transport parameterization. In this case, the inverse method was used to characterize the sorption process for each

Table 3
Goodness-of-fit measures for simulations and experimental data. -: non-computed; O: observation; $\overline{O}$: mean of observations; P: predicted value; j: total number of data points.

			C12			C14			C16			C18	
Soil core		θ	EO3	EO6	EO8	EO3	EO6	EO8	EO3	EO6	EO8	EO3	EO6	EO8
1	[a]*MAE*	0.03	1.17	1.57	2.08	0.15	0.67	1.47	–	1.27	–	–	3.83	5.71
	[b]*RMSE*	0.04	1.35	1.82	3.31	0.22	0.91	2.28	–	1.78	–	–	4.93	7.46
	[c]*E'*	0.76	−0.59	−0.94	0.02	0.34	−0.16	−0.11	–	−0.20	–	–	0.02	0.25
2	[a]*MAE*	0.02	–	1.65	8.84	0.14	0.62	0.36	0.15	0.53	0.60	0.12	1.03	4.43
	[b]*RMSE*	0.02	–	1.98	18.75	0.23	1.29	0.73	0.23	0.63	0.73	0.14	1.61	8.86
	[c]*E'*	0.68	–	−1.53	−8.18	0.11	−1.23	0.02	−0.02	0.28	0.53	0.31	0.53	0.35

[a] Mean absolute error. $MAE = \frac{\sum_{i=1}^{j}|O-P|}{j}$

[b] Root mean square error. $RMSE = \sqrt{\frac{1}{j}\sum_{i=1}^{j}(O-P)^2}$

[c] Modified coefficient of efficiency. $E' = 1 - \frac{\sum_{i=1}^{j}|O-P|}{\sum_{i=1}^{j}|O-\overline{O}|}$

surfactant under flow experimental conditions. Note that, due to the low concentrations used, the impact of surfactants on the hydraulic properties was discarded (*e.g.*, Kanokkarn et al., 2017). The kinetics of sorption and degradation (Table 2) were preestablished based on laboratory determinations and literature, respectively. Sorption kinetics (first order sorption rate coefficient) determined experimentally resulted very similar to previous estimations for similar compounds. The degradation constant values used (from Hermens and Droge, 2009) were slightly higher than the ones provided for similar compounds (*e.g.*, linear alcohol ethoxylates) and for a large variety of soils (Knaebel et al., 1990; Federle et al., 1997). This resulted in a slightly shorter half-life, *i.e.*, faster decay, which was expected in our soils as they have been previously exposed to surfactants and other sewage derived chemicals, and the microbial community might be already acclimated to this type of contaminants. Similar to the water flow model, the performance of the calibrated model was evaluated both in terms of goodness-of-fit to available total concentration (sorbed + dissolved) measurements and plausibility of the model parameters. Although the fit of the model for each surfactant was not as good as for soil water content, the reactive transport model captured quite well the shape of the total concentration profiles. Important differences between observed and simulated values were, however, systematically found for the sampling point at the surface (0 cm depth). This point lies at the interface between the applied water and the soil surface, and generally presents a high total AEO concentration, both experimentally and numerically. This fact evidences the difficulties in capturing the processes occurring at the atmosphere–soil boundary layer.

The obtained parameterization for the sorption process from both batch experiments and simulation of the infiltration experiments can be explained from the existing heterogeneity in the fluid flow at pore scale. From the simulation of the infiltration experiments, the fitted parameter K_d for each surfactant was ~1.5 orders of magnitude smaller than the values obtained from batch experiments (Traverso-Soto et al., 2014). During the initial imbibition phase no fingering (unstable flow) was observed. However, once steady-state conditions were reached, unsaturated flow in soil is still very heterogeneous, with the coexistence of high velocity regions (preferential paths) and low velocity regions or stagnation zones (De Gennes 1983; Jiménez-Martínez et al., 2015, 2017). This double flow structure (Holzner et al., 2015) reduces the surface contact between the contaminant and the solid particles, and therefore reduces the sorption capacity. For the other Freundlich isotherm parameter, β, there was much less discrepancy between estimates from batch experiments and simulated results from the infiltration experiments, with the exception of values for the EO3 AEOs, for which the measured range from batch experiments was wider than the simulated one. The β values (systematically < 1) of the adopted Freundlich isotherm, obtained from the simulation of the infiltration experiments, indicate an agreement with previous studies where the sorption of non-inonic surfactants in soils was described by a Langmuir isotherm (Lee et al., 2005). The low concentrations used in the infiltration experiments impeded to reach the sorption saturation. Note that Freundlich isotherms have also been determined for AEOs in other matrices such as receiving water solids (Van Compernolle et al., 2006). The comparison established here highlights the inappropriateness of using sorption parameters inferred from batch experiments in field-scale environmental studies.

When comparison was done considering the structural diversity of AEOs, values of K_d did not differ according to the carbon chain length, either in the values deduced from the batch experiments or simulated from the infiltration experiments. By ethoxylated groups, K_d from batch experiments using EO3 ethoxymers remained grouped and with a smaller average value, while EO6 and EO8 did not (Fig. 4b), having larger average values. This can be explained by the hydrogen bonding between EOs and functional groups on various soil components, which is the primary mechanism accounting for the preferential sorption of long EO homologs. Sorption of individual homologs within a mixture has been found for increasing as EOs number increases (Yuan and Jafvert, 1997). Consequently, higher values were expected for groups EO6 and EO8 than for EO3. The similar values observed for the simulated K_d as a function of both carbon chain length and ethoxymers can be explained by the low concentrations used in the infiltration experiments and the fast biodegradation, which can hide these differences. Estimates of β from batch experiments and in the simulations did not differ according to the length of the carbon chains or the number of ethoxylated groups, except for the measured value of β for EO3, which had a wider range of values than for the other ethoxymers. This difference between ethoxymers was not observed in the simulated β values, which can be equally explained by the lower concentrations used, and specially measured as sorbed in the infiltration experiments, and hide by the fast biodegradation.

It has been demonstrated that the sorption of non-ionic surfactants is proportional to the clay content unless the soil has a fairly high organic carbon content (Lee et al., 2005), as well as a larger affinity with organic substances as carbon chain length

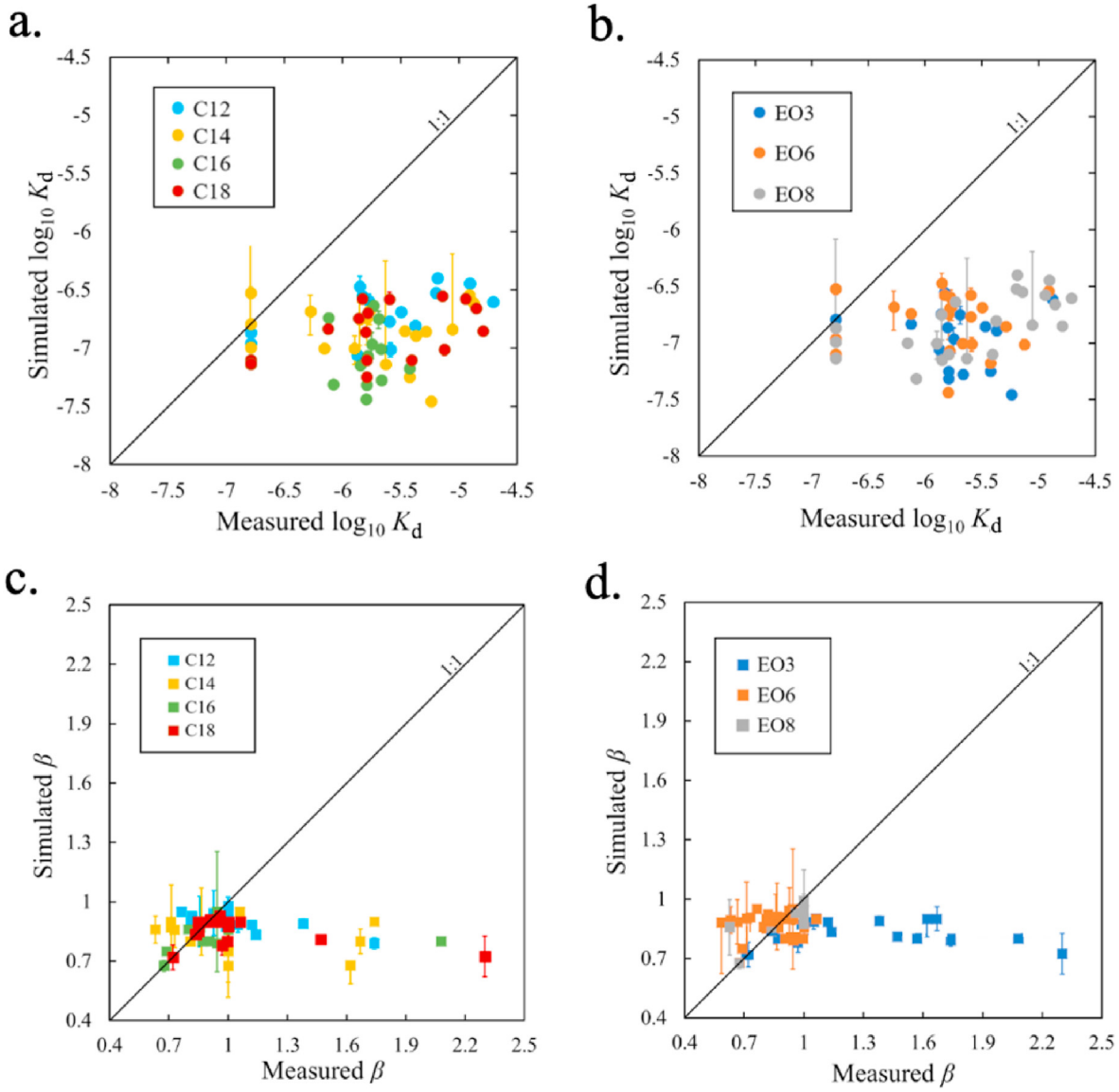

Fig. 4. (a,b) Values of K_d [cm^3/ng] (expressed as log10 K_d) from simulation of infiltration experiments plotted against values from batch experiments, with colors representing (a) the length of the carbon chain (C12, blue; C14, yellow; C16, green; and C18, red), and (b) the number of ethoxylated groups (EO3, blue; EO6, orange; and EO8, gray). (c,d) Values of β from simulation of infiltration experiments plotted against values from batch experiments, with colors representing (c) the length of the carbon chain (C12, blue; C14, yellow; C16, green; and C18, red), and (d) the number of ethoxylated groups (EO3, blue; EO6, orange; and EO8, gray). Error bars indicate 95% confidence intervals for the calibrated parameters. (For interpretation of the references to color in this figure legend, the reader is referred to the Web version of this article.)

increases as compared with the number of ethoxylate groups (McAvoy and Kerr, 2001). For the AEOs studied, no clear dependence of K_d on clay content by number of ethoxylated groups and on organic carbon content by carbon chain length was observed (Shen, 2000; Traverso-Soto et al., 2014). Differences existed, however, between batch experiments and simulated values in the relationship between K_d values and the two soil properties. The value of K_d reached an asymptote for clay content > 1%, while simulated values remained more or less constant independent of the clay content. Similar behavior is observed for K_d as function of organic carbon content, with an asymptote above an organic carbon content of 0.3%. Both clay and organic carbon content of the used soils were relatively low, which can explain the no clear trend of K_d values obtained from both batch experiments and simulated from the infiltration experiments. The low clay and organic carbon content of the studied soils explains the lack of a strong correlation of sorption capacity with any of these soil properties (Fig. 5). The simultaneous biodegradation of AEOs, as observed for similar surfactants (Knaebel et al., 1990) under the experimented aerobic conditions, can hide these differences.

Of the total mass of each surfactant applied, up to 99% was sorbed and/or degraded, being sorption the dominant process in the soil core 1 (slow flow conditions), and the lower sorption in the soil core 2 (fast flow conditions) was counterbalance by the significant degradation. Less than 0.5% of surfactants mass percolated through to the bottom of the flow cell. Although the sorption capacity is reduced considerably (by more than one order of magnitude) under environmental conditions with flow, thereby increasing the potential percolation depth, the rapid degradation, including due to biodegradation (Brownawell et al., 1997; Cano and Dorn, 1996), and the expected thicker unsaturated zone (more than the height of the flow cell used) minimizes the risk of the

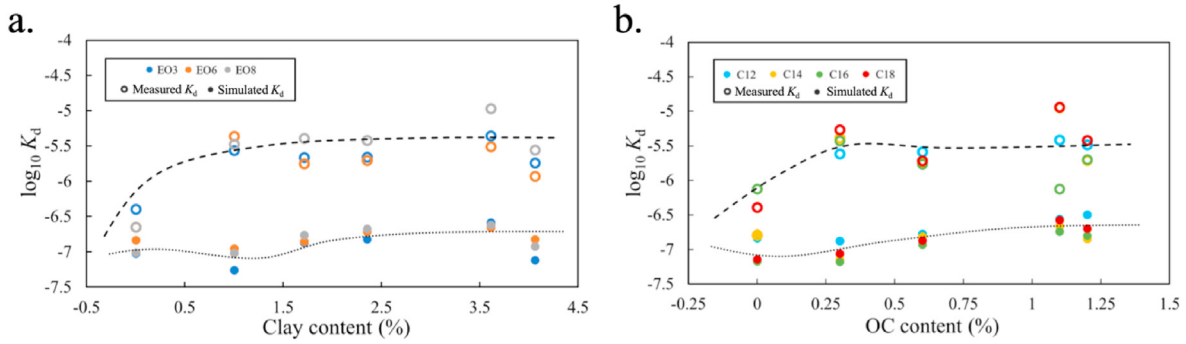

Fig. 5. (a) Average $\log_{10} K_d$ values measured in batch experiments (empty circles) and simulated from the infiltration experiments (filled circles) as a function of clay content (%), plotted according to the number of ethoxylated groups: EO3 (blue), EO6 (orange) and EO8 (gray). (b) Average $\log_{10} K_d$ values measured in batch experiments (empty circles) and simulated from the infiltration experiments (filled circles) as a function of organic carbon content (OC %), plotted according to the carbon chain length: C12 (blue), C14 (yellow), C16 (green) and C18 (red). The dashed and dotted lines represent the moving average for batch and simulated K_d values, respectively. (For interpretation of the references to color in this figure legend, the reader is referred to the Web version of this article.)

contamination of groundwater bodies by AEOs. Similar results have been obtained for anionic surfactants (*e.g.*, LAS) from percolation experiments, in which beyond a retention favored by higher clay and organic carbon contents especially for longer-chain homologs, a significant biodegradation reduced the deep percolation (Küchler and Schnaak, 1997; Boluda et al., 2010).

5. Conclusions

The methodology we apply here, combining sorption isotherms obtained from batch experiments, longitudinal distribution profiles for AEO concentrations using infiltration experiments, and numerical simulations, demonstrate the need to be cautious when using the isotherms obtained from batch experiments to assess the risk to subsurface environments imposed by non-ionic surfactants. The resulting K_d coefficients for non-ionic surfactants under flow/natural conditions, and inferred from inverse numerical simulations, were 1–2 orders of magnitude lower than those obtained from batch experiments, independently of the homolog (*i.e.*, carbon chain length and the number of ethoxylated groups). No clear trends for K_d as a function of clay and organic carbon content were observed, independently of the homolog. Therefore, further studies with higher concentration of contaminants, mimicking a punctual source, are recommended in order to better characterize the fate and transport of non-ionic surfactant homologs, and in particular the impact of clay and organic carbon content on the sorption process in soils, reducing the uncertainty in predictive models and the risk of contamination of groundwater bodies.

Author statement

Marta Botella Espeso: Formal analysis, Data curation, Methodology, Writing - original draft. **Carmen Corada-Fernández:** Formal analysis, Data curation, Methodology, Writing - review & editing. **Maider García-Delgado:** Formal analysis, Data curation, Methodology. **Lucila Candela:** Funding acquisition, Writing - original draft. **Eduardo González-Mazo:** Funding acquisition, Writing - original draft. **Pablo A. Lara-Martín:** Writing - original draft, Writing - review & editing. **Joaquín Jiménez-Martínez:** Conceptualization, Funding acquisition, Supervision, Writing - original draft, Writing - review & editing.

Declaration of competing interest

The authors declare that they have no known competing financial interests or personal relationships that could have appeared to influence the work reported in this paper.

Acknowledgements

We thank Emiliano M. Gómez (SCCYT UCA) for his technical assistance with the LC/MS. The work was carried out as part of the CGL 2008-05598 project, funded by the Spanish Ministry of Science and Technology (CICYT). M.B.E. and J.J.-M. gratefully acknowledge the Lifelong Learning Programme – Freemover Scholarship (European Commission). J.J.-M. gratefully acknowledges the financial support from the Swiss National Science Foundation (SNSF, grant Nr. 200021_178986). The authors acknowledge fruitful discussions about the experiments with J.E. Smith (McMaster University) and about the numerical simulations with M. Vanclooster (Université Catholique de Louvain). We thank the anonymous reviewers and the editor whose valuable comments and suggestions help to improve the manuscript.

Appendix A. Supplementary data

Supplementary data to this article can be found online at https://doi.org/10.1016/j.envpol.2020.116021.

References

Adeel, Z., Luthy, R.G., 1995. Concentration-dependent regimes in sorption and transport of a nonionic surfactant in sand—aqueous systems. Surfactant-Enhanced Subsurface Remediation, 594. American Chemical Society, pp. 38–53.
Ahel, M., Schaffner, C., Giger, W., 1996. Behaviour of alkylphenol polyethoxylate surfactants in the aquatic environment-III. Occurrence and elimination of their persistent metabolites during infiltration of river water to groundwater. Water Res. 30 (1), 37–46.
Bear, J., 1972. Dynamics of Fluids in Porous Media. Dover Publications, Inc, New York.
Biel-Maeso, M., Corada-Fernández, C., Lara-Martín, P.A., 2017. Determining the distribution of pharmaceutically active compounds (PhACs) in soils and sediments by pressurized hot water extraction (PHWE). Chemosphere 185, 1001–1010.
Boluda-Botella, N., León, V.M., Cases, V., Gomis, V., Prats, D., 2010. Fate of linear alkylbenzene sulfonate in agricultural soil columns during inflow of surfactant pulses. J. Hydrol. 395 (3–4), 141–152.
Brownawell, B.J., Chen, H., Zhang, W., Westall, J.C., 1997. Sorption of nonionic surfactants on sediment materials. Environ. Sci. Technol. 31 (6), 1735–1741.
Cano, M., Dorn, P., 1996. Sorption of two model alcohol ethoxylate surfactants to sediments. Chemosphere 33 (6), 981–994.
Carlsen, L., Metzon, M.B., Kjelsmark, J., 2002. Linear alkylbenzene sulfonates (LAS) in the terrestrial environment. Sci. Total Environ. 290 (1–3), 225–230.
Connors, K.A., 1990. Chemical Kinetics: the Study of Reaction Rates in Solution. John Wiley & Sons.
Corada-Fernández, C., Lara-Martín, P.A., Candela, L., González-Mazo, E., 2011. Tracking sewage derived contamination in riverine settings by analysis of

synthetic surfactants. J. Environ. Monit. 13 (7), 2010–2017.
Corada-Fernández, C., Lara-Martín, P.A., Candela, L., González-Mazo, E., 2013. Vertical distribution profiles and diagenetic fate of synthetic surfactants in marine and freshwater sediments. Sci. Total Environ. 461, 568–575.
Corada-Fernández, C., Jiménez-Martínez, J., Candela, L., González-Mazo, E., Lara-Martín, P.A., 2015. Occurrence and spatial distribution of emerging contaminants in the unsaturated zone. Case study: guadalete River basin (Cadiz, Spain). Chemosphere 119, S131–S137.
Corada-Fernández, C., Candela, L., Torres-Fuentes, N., Pintado-Herrera, M.G., Paniw, M., González-Mazo, E., 2017. Effects of extreme rainfall events on the distribution of selected emerging contaminants in surface and groundwater: the Guadalete River basin (SW, Spain). Sci. Total Environ. 605, 770–783.
De Gennes, P.G., 1983. Hydrodynamic dispersion in unsaturated porous media. J. Fluid Mech. 136, 189–200.
Ding, W.H., Tzing, S.H., Lo, J.H., 1999. Occurrence and concentrations of aromatic surfactants and their degradation products in river waters of Taiwan. Chemosphere 38 (11), 2597–2606.
Droge, S.T., Hermens, J.L., 2007. Nonlinear sorption of three alcohol ethoxylates to marine sediment: a combined Langmuir and Linear sorption process? Environ. Sci. Technol. 41 (9), 3192–3198.
Droge, S.T., Hermens, J.L., 2010. Alcohol ethoxylate mixtures in marine sediment: competition for adsorption sites affects the sorption behaviour of individual homologues. Environ. Pollut. 158 (10), 3116–3122.
Droge, S.T., Yarza-Irusta, L., Hermens, J.L., 2009. Modeling nonlinear sorption of alcohol ethoxylates to sediment: the influence of molecular structure and sediment properties. Environ. Sci. Technol. 43 (15), 5712–5718.
Durán-Álvarez, J.C., Sánchez, Y., Jiménez, B., Prado, B., 2014. The transport of three emerging pollutants through an agricultural soil irrigated with untreated wastewater. J. Water Reuse Desal. 4 (1), 1–9.
Eadsforth, C.V., Sherren, A.J., Selby, M.A., Toy, R., Eckhoff, W.S., McAvoy, D.C., Matthijs, E., 2006. Monitoring of environmental fingerprints of alcohol ethoxylates in Europe and Canada. Ecotoxicol. Environ. Saf. 64 (1), 14–29.
Eichhorn, P., Silvana, V., Rodrigues, S.V., Baumann, W., Knepper, T.P., 2002. Incomplete degradation of linear alkylbenzene sulfonate surfactants in Brazilian surface waters and pursuit of their polar metabolites in drinking waters. Sci. Total Environ. 284 (1–3), 123–134.
El Rayis, O., 1985. Re-assessment of the titration method for determination of organic carbon in recent sediments. Rapp. Comm. Int. Mer. Medit. 29, 45–47.
El-Kadi, A.I., Ling, G., 1993. The Courant and Peclet number criteria for the numerical solution of the Richards equation. Water Resour. Res. 29 (10), 3485–3494.
Federle, T.W., Gasior, S.D., Nuck, B.A., 1997. Extrapolating mineralization rates from the ready CO2 screening test to activated sludge, river water, and soil. Environ. Toxicol. Chem. 16 (2), 127–134.
Ferguson, P.L., Iden, C.R., Brownawell, B.J., 2001. Distribution and fate of neutral alkylphenol ethoxylate metabolites in a sewage-impacted urban estuary. Environ. Sci. Technol. 35 (12), 2428–2435.
Garcia, R.A., Chiaia-Hernández, A.C., Lara-Martín, P.A., Loos, M., Hollender, J., Oetjen, K., Higgins, C.P., Field, J.A., 2019. Suspect screening of hydrocarbon surfactants in AFFFs and AFFF-contaminated groundwater by high resolution mass spectrometry. Environ. Sci. Technol. 53 (14), 8068–8077.
Gaudette, H., Flight, W., Torner, L., Folger, D.W., 1974. An inexpensive titration method for the determination of organic carbon in recent sediments. J. Sediment. Res. 44 (1), 249–253.
Gee, G., Or, D., 2002. Particle size analysis. Methods of Soil Analysis. Volume Part 4, SSSA Book Series, vol. 5. Am. Soc. Agron., Madison, WI, pp. 255–294.
González-Mazo, E., Forja, J.M., Gómez-Parra, A., 1998. Fate and distribution of linear alkylbenzene sulfonates in the littoral environment. Environ. Sci. Technol. 32 (11), 1636–1641.
González-Mazo, E., León, V.M., Sáez, M., Gómez-Parra, A., 2002. Occurrence and distribution of linear alkylbenzene sulfonates and sulfophenylcarboxylic acids in several Iberian littoral ecosystems. Sci. Total Environ. 288 (3), 215–226.
Grossman, R.B., Reinsch, T., 2002. Bulk Density and Linear Extensibility. Methods of Soil Analysis, Volume Part 4. Am. Soc. Agron., Madison, WI, pp. 201–228. SSSA Book Series: 5.
Guang-Guo, Y., 2006. Fate, behavior and effects of surfactants and their degradation products in the environment. Environ. Int. 32 (3), 417–431.
Haigh, S.D., 1996. A review of the interaction of surfactants with organic contaminants in soil. Sci. Total Environ. 185 (1–3), 161–170.
Hermens, J.L., Droge, S.T., 2009. Human and Environmental Risk Assessment on Ingredients of European Household Cleaning Products, HERA. Alcohol Ethoxylates (AEOs), pp. 1–14 (Brussels, Belgium).
Holzner, M., Morales, V.L., Willmann, M., Dentz, M., 2015. Intermittent Lagrangian velocities and accelerations in three-dimensional porous medium flow. Phys. Rev. E. https://doi.org/10.1103/PhysRevE.92.013015.
Jiménez-Martínez, J., de Anna, P., Tabuteau, H., Turuban, R., Le Borgne, T., Méheust, Y., 2015. Pore scale mechanisms for the enhancement of mixing in unsaturated porous media and implications for chemical reactions. Geophys. Res. Lett. 42 (13), 5316–5324.
Jiménez-Martínez, J., Le Borgne, T., Tabuteau, H., Méheust, Y., 2017. Impact of saturation on dispersion and mixing in porous media: photo-bleaching pulse injection experiments and shear-enhanced mixing model. Water Resour. Res. 53 (2), 1457–1472.
John, D.M., House, W.A., White, G.F., 2009. Environmental fate of nonylphenol ethoxylates: differential adsorption of homologs to components of river sediment. Environ. Toxicol. Chem. 19 (2), 293–300.
Jonkers, N., Laane, R.W., de Voogt, P., 2003. Fate of nonylphenol ethoxylates and their metabolites in two Dutch estuaries: evidence of biodegradation in the field. Environ. Sci. Technol. 37 (2), 321–327.
Kanokkarn, P., Shiina, T., Santikunaporn, M., Chavadej, S., 2017. Equilibrium and dynamic surface tension in relation to diffusivity and foaming properties: effects of surfactant type and structure. Colloid. Surf. A Physicochem. Eng. Asp. 524, 135–142.
Kiewiet, A., de Beer, K.G.M., Parsons, J.R., Govers, H.A.J., 1996. Sorption of linear alcohol ethoxylates on suspended sediment. Chemosphere 32 (4), 675–680.
Knaebel, D.B., Vestal, J.R., Federle, T.W., 1990. Mineralization of linear alkylbenzene sulfonate (LAS) and linear alcohol ethoxylate (LAE) in 11 contrasting soils. Environ. Toxicol. Chem. 9 (8), 981–988.
Krueger, C., Radakovich, K., Sawyer, T., Barber, L.B., Smith, R.L., Field, J., 1998. Biodegradation of the surfactant linear alkylbenzenesulfonate in sewage-contaminated groundwater: a comparison of column experiments and field-tracer tests. Environ. Sci. Technol. 32, 3954–3961.
Küchler, T., Schnaak, W., 1997. Behaviour of linear alkylbenzene sulphonates (LAS) in sandy soils with low amounts of organic matter. Chemosphere 35 (1–2), 153–167.
Lara-Martín, P.A., Gómez-Parra, A., González-Mazo, E., 2006. Development of a method for the simultaneous analysis of anionic and non-ionic surfactants and their carboxylated metabolites in environmental samples by mixed-mode liquid chromatography–mass spectrometry. J. Chromatogr. A 1137 (2), 188–197.
Lara-Martín, P.A., Gómez-Parra, A., González-Mazo, E., 2008. Sources, transport and reactivity of anionic and non-anionic surfactants in several aquatic ecosystems from SW of Spain: a comparative study. Environ. Pollut. 156 (1), 36–45.
Lara-Martín, P.A., González-Mazo, E., Brownawell, B.J., 2011. Multi-residue method for the analysis of synthetic surfactants and their degradation metabolites in aquatic systems by liquid chromatography–time-of-flight-mass spectrometry. J. Chromatogr. A 1218 (30), 4799–4807.
Lara-Martín, P.A., González-Mazo, E., Brownawell, B.J., 2012. Environmental analysis of alcohol ethoxylates and nonylphenol ethoxylate metabolites by ultra-performance liquid chromatography–tandem mass spectrometry. Anal. Bioanal. Chem. 402 (7), 2359–2368.
Lara-Martín, P.A., González-Mazo, E., Petrovic, M., Barceló, D., Brownawell, B.J., 2014. Occurrence, distribution and partitioning of nonionic surfactants and pharmaceuticals in the urbanized Long Island Sound Estuary (NY). Mar. Pollut. Bull. 85 (2), 710–719.
Lara-Martín, P.A., Gómez-Parra, A., González-Mazo, E., 2005. Determination and distribution of alkyl ethoxysulfates and linear alkylbenzene sulfonates in coastal marine sediments from the Bay of Cadiz (southwest of Spain). Environ. Toxicol. Chem. 24 (9), 2196–2202.
Lee, J.F., Liao, P.M., Kuo, C.C., Yang, H.T., Chiou, C.T., 2000. Influence of a nonionic surfactant (Triton X-100) on contaminant distribution between water and several soil solids. J. Colloid Interface Sci. 229 (2), 445–452.
Lee, J.F., Hsu, M.H., Lee, C.K., Chao, H.P., Chen, B.H., 2005. Effects of soil properties on surfactant adsorption. J. Chin. Inst. Eng. 28 (2), 375–379.
Legates, D.R., McCabe, G.J., 1999. Evaluating the use of "goodness-of-fit" measures in hydrologic and hydroclimatic model validation. Water Resour. Res. 35, 233–241.
León, V.M., González-Mazo, E., Pajares, J.M.F., Gómez-Parra, A., 2001. Vertical distribution profiles of linear alkylbenzene sulfonates and their long-chain intermediate degradation products in coastal marine sediments. Environ. Toxicol. Chem. 20 (10), 2171–2178.
Matthijs, E., Holt, M.S., Kiewiet, A., Rijs, G.B., 1999. Environmental monitoring for linear alkylbenzene sulfonate, alcohol ethoxylate, alcohol ethoxy sulfate, alcohol sulfate, and soap. Environ. Toxicol. Chem. 18 (11), 2634–2644.
McAvoy, D.C., White, C.E., Moore, B.L., Rapaport, R.A., 1994. Chemical fate and transport in a domestic septic system: sorption and transport of anionic and cationic surfactants. Environ. Toxicol. Chem. 13 (2), 213–221.
McAvoy, D.C., Dyer, S.D., Fendinger, N.J., Eckhoff, W.S., Lawrence, D.L., Begley, W.M., 1998. Removal of alcohol ethoxylates, alkyl ethoxylate sulfates, and linear alkylbenzene sulfonates in wastewater treatment. Environ. Toxicol. Chem. 17 (9), 1705–1711.
McAvoy, D.C., Kerr, K.M., Clapp, C.E., Hayes, M.H.B., Senesi, N., Bloom, P.R., Jardine, P.M., 2001. In: Association of Alcohol Ethoxylates with a Dissolved Humic Substance. *Humic Substances and Chemical Contaminants*. ASA, CSSA, and SSSA Books, pp. 177–186. Book Series.
Millington, R.J., Quirk, J., 1961. Permeability of porous solids. Trans. Faraday Soc. 57, 1200–1207.
Montgomery-Brown, J., Drewes, J.E., Fox, P., Reinhard, M., 2003. Behavior of alkylphenol polyethoxylate metabolites during soil aquifer treatment. Water Res. 37 (15), 3672–3681.
Morrall, S., Eckhoff, W.S., Evans, A., Cano, M.L., Dunphy, J.C., McAvoy, D.C., 2006. Removal of alcohol ethoxylates and environmental exposure determination in the United States. Ecotoxicol. Environ. Saf. 64 (1), 3–13.
Mualem, Y., 1976. Hysteretical models for prediction of the hydraulic conductivity of unsaturated porous media. Water Resour. Res. 12 (6), 1248–1254.
Nash, J.E., Sutcliffe, J.V., 1970. River flow forecasting through conceptual models, part I: a discussion of principles. J. Hydrol. 10, 282–290.
Petrovic, M., Fernández-Alba, A.R., Borrull, F., Marce, R.M., Mazo, E.G., Barceló, D., 2002. Occurrence and distribution of nonionic surfactants, their degradation products, and linear alkylbenzene sulfonates in coastal waters and sediments in Spain. Environ. Toxicol. Chem. 21 (1), 37–46.
Podoll, R.T., Irwin, C.C., Brendlinger, S., 1987. Sorption of water-soluble oligomers on

sediments. Environ. Sci. Technol. 21 (6), 562–568.
Reynolds, W., Elrick, D., 2002. Hydraulic conductivity of saturated soils, constant head method. In: Methods of Soil Analyses. Physical Methods, Book Series 5. Soil Science Society of America, Madison, WI, pp. 697–700.
Ritter, A., Muñoz-Carpena, R., 2013. Performance evaluation of hydrological models: statistical significance for reducing subjectivity in goodness-of-fit assessments. J. Hydrol. 480, 33–45.
Schaap, M.G., Leij, F.J., van Genuchten, M. Th, 2001. ROSETTA: a computer program for estimating soil hydraulic parameters with hierarchical pedotransfer functions. J. Hydrol. 251 (3–4), 163–176.
Shen, Y.H., 2000. Sorption of non-ionic surfactants to soil: the role of soil mineral composition. Chemosphere 41 (5), 711–716.
Šimůnek, J., Van Genuchten, M.Th, Sejna, M., 2015. The HYDRUS-1D Software Package for Simulating the One-Dimensional Movement of Water, Heat, and Multiple Solutes in Variably-Saturated Media. Department of Environmental Sciences, University of California Riverside, Riverside, CA, USA.
Smith, J.E., Gillham, R.W., 1994. The effect of concentration-dependent surface tension on the flaw of water and transport of dissolved organic compounds: a pressure head-based formulation and numerical model. Water Resour. Res. 30 (2), 343–354.
Smith, J.E., Gillham, R.W., 1999. Effects of solute concentration–dependent surface tension on unsaturated flow: laboratory sand column experiments. Water Resour. Res. 35 (4), 973–982.
Song, Q., Couzis, A., Somasundaran, P., Maldarelli, C., 2006. A transport model for the adsorption of surfactant from micelle solutions onto a clean air/water interface in the limit of rapid aggregate disassembly relative to diffusion and supporting dynamic tension experiments. Colloid. Surface. A 282, 162–182.
Szymanski, A., Wyrwas, B., Lukaszewski, Z., 2003. Determination of non-ionic surfactants and their biotransformation by-products adsorbed on alive activated sludge. Water Res. 37 (2), 281–288.
Topp, E., Metcalfe, C., Edwards, M., Payne, M., Kleywegt, S., Russell, P., Lapen, Gottschall, N., 2012. Pharmaceutical and personal care products in groundwater, subsurface drainage, soil, and wheat grain, following a high single application of municipal biosolids to a field. Chemosphere 87 (2), 194–203.
Traverso-Soto, J.M., Brownawell, B.J., González-Mazo, E., Lara-Martín, P.A., 2014. Partitioning of alcohol ethoxylates and polyethylene glycols in the marine environment: field samplings vs laboratory experiments. Sci. Total Environ. 490, 671–678.
Tubau, I., Vázquez-Suñé, E., Carrera, J., González, S., Petrovic, M., López de Alda, M.J., Barceló, D., 2010. Occurrence and fate of alkylphenol polyethoxylate degradation products and linear alkylbenzene sulfonate surfactants in urban ground water: barcelona case study. J. Hydrol. 383 (1–2), 102–110.
Van Compernolle, R., McAvoy, D.C., Sherren, A., Wind, T., Cano, M.L., Belanger, S.E., Dorn, P.B., Kerr, K.M., 2006. Predicting the sorption of fatty alcohols and alcohol ethoxylates to effluents and receiving water solids. Ecotoxicol. Environ. Saf. 64 (1), 61–74.
Van Genuchten, M.Th, 1980. A closed-form equation for predicting the hydraulic conductivity of unsaturated soils 1. Soil Sci. Soc. Am. J. 44, 892–898.
Vanderborght, J., Vereecken, H., 2007. Review of dispersivities for transport modeling in soils. Vadose Zone J. 6 (1), 29–52.
Vanderborght, J., Kasteel, R., Herbst, M., Javaux, M., Thiéry, D., Vanclooster, M., Mouvet, C., Vereecken, H., 2005. A set of analytical benchmarks to test numerical models of flow and transport in soils. Vadose Zone J. 4 (1), 206–221.
Wind, T., Stephenson, R.J., Selby, M.A., Eadsforth, C.V., Sherren, A.J., Toy, R., 2006. Determination of the fate of alcohol ethoxylate homologs in a laboratory continuous activated-sludge unit study. Ecotoxicol. Environ. Saf. 64, 42–60.
Yuan, C., Jafvert, C.T., 1997. Sorption of linear alcohol ethoxylate surfactant homologs to soils. J. Contam. Hydrol. 28 (4), 311–325.